

## Strain behaviour of thin film PZT (30/70) examined through Piezo-force microscopy (P-AFM)

S. Dunn\*

Building 70, Nanotechnology, Cranfield University, Cranfield, MK43 0AL, UK

\* corresponding author; S Dunn, s.c.dunn@cranfield.ac.uk

### Abstract

Using an atomic force microscope (AFM) modified to perform PiezoAFM we have investigated the piezoelectric response of sol-gel thin film lead zirconate titanate (PZT 30/70,  $\text{PbZr}_{0.3}\text{Ti}_{0.7}\text{O}_3$ ) on Pt-Ti/SiO<sub>2</sub>/Si to a quasi DC electric field. The films were produced by spin coating a PZT 30/70 sol onto a selected substrate and firing at 520°C. This generated a film that was highly [111] orientated and single phase perovskite. By applying a sinusoidal 2Hz AC waveform between the AFM cantilever and ground we have generated strain-field, or butterfly loops for the PZT film. PiezoAFM butterfly loops show that the localised piezoelectric response for PZT varies depending on the sign of the applied field. The degree of asymmetry in the hysteresis loop has been attributed to charge trapping at the electrode-PZT interface generating a system that can preferentially re-pole in one direction. The charge trapped at the interface has an overwhelming effect on the polarisability of the film. Coercive fields have been calculated from the minimum point of the strain before reversal for the system and are shown to be  $-30\text{V}/\mu\text{m}$  and  $+32\text{V}/\mu\text{m}$  in absolute terms and  $-23\text{V}/\mu\text{m}$  and  $+39\text{V}/\mu\text{m}$  in terms relative to the charge trapped at the electrode interface.  $\delta_{33}$  values obtained for the PZT thin film

investigated ranged from 30 to 40pm/V. The maximum strain of the system was shown at applied biases of +/-10V and was 0.3% at a bias of +10V, although at this field the sample was not showing saturated behaviour. By relating the offset of the butterfly loops to the charge density generated by defects at the PZT-electrode interface, calculated to be  $0.025\text{Cm}^{-2}$ , an estimate of the number of defects at the interface has been drawn. The concentration of defects at the interface is 1 defect for every  $6\text{nm}^2$  of surface, representing 1 defect for every 40 unit cells or 2.5% of unit cells being defected.

## Introduction

Ferroelectric materials such as lead zirconate titanate ( $\text{PbZr}_x\text{Ti}_{1-x}\text{O}_3$ , PZT) have been undergoing increasing study in recent years, as their suitability for use in non-volatile memories<sup>1-3</sup> and other MEMS<sup>4-8</sup> applications has been recognised. The development of techniques, such as sol-gel, that allow the production of very highly orientated thin film PZT at temperatures compatible with standard Si fabrication techniques has further enhanced this interest<sup>9-13</sup>. For devices to be made successfully the ferroelectric material produced should be high quality with a minimum of rosettes and, for many applications, highly [111] orientated<sup>14</sup>. The generation of a ferroelectric material that is highly repeatable in terms of ferroelectric performance is very desirable.

The scale of interest for the grain and domain structures is now sub-micron<sup>15</sup>. Standard analytical techniques do not allow the determination of ferroelectric properties at this scale. The development of atomic force microscopy has allowed the routine evaluation of surface topography of these materials, and in the last few years a number of additional techniques have been developed. Prime among these for determining the

ferroelectric properties of a material is piezoelectric atomic force microscopy (P-AFM)<sup>16-20</sup>. P-AFM detects the converse piezoelectric response of the material under investigation and allows the mapping of the ferroelectric domains, the generation of highly localised hysteresis loops and the production of strain-field (butterfly) loops. The use of an AFM tip as a small and moveable conductive probe has reduced the scale of the study of piezoelectricity to just a few tens of nanometers. Using P-AFM it is possible to map ferroelectric domains in a film without a top electrode and without altering them<sup>21</sup>.<sup>22</sup>. The technique described in this paper also allows the strain behaviour of the material to be determined in the absence of a top electrode with the obvious advantages that the sample can be reworked and the possibility of having the same top electrode structure as that on the bottom. This advantage allows for electrodes with the same work function to be evaluated and hence asymmetry in hysteresis loops is not caused by preferential injection of electrons but by inherent features of the films.

When the drive voltage applied to the sample is stepped from one drive amplitude (such as 5V to 6V) to another the sample was left for a period of between 10 and 15 minutes in order to eliminate drift. Drift in the image obtained was always seen for the first few minutes after changing the drive voltage.

## Experimental

A schematic of the experimental arrangement used to perform PFM is shown in Figure 1. A sinusoidal voltage was passed between the AFM tip and the back electrode of the PZT sample, usually held at ground. The signal used in all cases was 2Hz with a variation in the amplitude (from -10V to +10V) to investigate the displacement generated in the sample. During the experiment the scan size was set to 0nm in order to remove

any topographic variation from the z-axis displacement with a scan rate of 2Hz. The displacement of the sample surface due to the applied field was directly interpreted from the z-axis scale of the microscope. The microscope used was a Digital Instruments 3000 systems with series III controller. The variation in the z-axis displacement was plotted against the applied field and can be interpreted as a typical strain/field plot for the sample. In this paper we use the term  $\delta_{33}$  to describe the piezoelectric response of the ferroelectric film under investigation. The tips used for the experiment were standard oxide sharpened Si probes with a spring constant of 0.02 to 0.1 N/m. These tips were coated with Ti(2nm)/Pt(5nm) in order to generate the same electrode structure on the tip as the back electrode of the ferroelectric sample. Great care was taken during the electroding of the tips to ensure that they were free of stress. PZT films with  $x = 0.3$  (PZT 30/70) were prepared using a sol-gel technique that has been described previously<sup>23, 24</sup>. The films were fired at two temperatures. Initially, a pyrolysis temperature of 200°C for 30 seconds was used. A final phase transformation temperature of 520°C with a dwell of 5 minutes completed the transformation to the perovskite phase.

## Results and discussion

### Calculation of piezoelectric constants

An example of a typical 'Scope trace' capture obtained from the microscope is shown in Figure 2. The 'scope trace' represents z-axis displacement against applied AC drive voltage for the PZT which the SPM generates for one line of scanning in the fast scan direction. There are two lines on the trace as the SPM captures both a trace and retrace scan. For this experiment the scan size has been set to 0nm, and so the y-axis of the scope trace is equivalent to time. The variation in the z-axis displacement obtained from

the surface of the sample is the true variation in displacement that the surface is exhibiting due to the converse piezoelectric effect. The lack of noise and drift in the sample is typical of a sample that has been allowed to stabilise for ca. 15 minutes after a variation in the applied field. The image was obtained at  $\pm 10\text{V}$  and  $2\text{Hz}$  and shows that the cantilever is displaced by approximately  $0.6\text{nm}$  during each cycle. The low value of this displacement along with the asymmetry in the response to the positive and negative applied fields is in contrast to the result shown in Figure 3. The displacement of the cantilever in Figure 3 is not being driven by the converse piezoelectric effect but by electrostatic repulsion between the cantilever and the surface. The large displacements ( $\pm 25\text{nm}$ ) for a film that is  $500\text{nm}$  thick are indicative of a sample that has a poor tip-surface contact or is not correctly grounded. Figure 4 shows a typical scope trace that is obtained when the sample is cycled through  $\pm 7\text{V}$  at  $2\text{Hz}$  and shows the increased noise due to the lower amplitude of displacement of the cantilever. Figure 4 also shows a significant amount of drift in the signal over time, this capture was taken after only 1 minute after a change in applied bias and is typical of the signal obtained before the system has stabilised.

Figure 5 presents a set of 'butterfly loops' for the PZT sample. Where, the applied bias is varied from  $\pm 7$  to  $\pm 10\text{V}$ . It was not possible to get data for a sample being driven with a bias of  $\pm 6\text{V}$ , because the data was swamped by the noise in the system. The loops show that even at the applied biases of  $\pm 10\text{V}$  the ferroelectric material is not saturating and that a full loop is starting to form at biases of  $\pm 8\text{V}$ , or more. The displacement of the 'butterfly loops' with respect to the origin in the field axis is believed to be due to the trapped charge at the electrode-PZT interface. There has been much speculation in the literature as to the exact nature of the trapped charge at the interface<sup>8, 25-30</sup>. It is generally agreed that this charge takes the form of oxygen defects, generating an inherent positive

charge at the interface. The variation in coercive field found in this work, and the associated variation in shape of the butterfly loops, supports that theory. When applying a positive field to the top surface of the PZT the initial orientation of dipoles is positive up. The negative end of the dipole (towards the bottom electrode) is stabilised by the positive field at the electrode interface meaning that the coercive field is higher. In absolute terms, the coercive field is found to be similar for both negative and positive fields (ca.  $30\text{V}/\mu\text{m}$ ). However, when the displacement in electric field due to the positive electric field at the back electrode is considered, the coercive fields become  $+39\text{V}/\mu\text{m}$  and  $-23\text{V}/\mu\text{m}$ . The values obtained lie close to those for other PZT films grown on similar substrates that have been examined using either PFM and on Radiant Technologies equipment. These values, of coercive field, reflect the sensitivity of the dipoles in the domains to all external electric fields, including those generated at the electrode PZT interface. The maximum strain achieved for the sample was ca 0.3% at +10V of applied bias. This value is consistent with that expected for a fully clamped PZT thin film.

It is interesting to note that the point at which the butterfly loop crosses itself varies as a function of applied bias. There is no shift in this 'origin' position until biases of 9V, or more, are applied. After this bias the 'origin' point shifts to the right, indicating that there is a reduction in the bias at the interface. The sample was run for a number of cycles (10 minutes or more) at each bias and the data shown represents a 'capture' that was made towards the end of the cycling period. No estimate can be made as to the dynamics of the inherent bias movement but it is interesting that as the sample begins to show fully open loops the inherent bias of the sample shifts to a more neutral position. This may be associated with the increase in the applied field which is capable of moving defects

through the lattice and thereby reducing the density of the defects. Or it may be due to a restructuring of the crystal after reversal of the domains and polling in both directions.

The relative 'openness' of the loop, which is found to be more open and nearer saturation for the positive applied field indicates that the mechanism dictating domain reversal lies more in the nucleation kinetics/dynamics than on the absolute field applied. The reason for this is that the effective field applied during the negative bias cycle is larger than during the positive cycle. The potential difference between a plate held at a positive bias and a negative electrode is higher than that between a plate held at ground and the same negative electrode, but the strain developed in the system and the degree of openness of the loops is less for negative cycles than positive ones.

It is possible to use a butterfly loop to determine the piezoelectric coefficients for a sample. In this case we do not give the piezoelectric coefficients as  $d_{33}$  values but as  $\delta_{33}$  as the method for analysis does not strictly conform to IEEE standards. By plotting the region of the butterfly loop that has a constant slope when crossing the 0 applied bias region it is possible to determine the  $d_{33}$  from the slope. In this case the slope of the plot is equivalent to the  $\delta_{33}$  for the sample. This has been done for all four applied bias's and is shown in Table 1, indicating that the  $\delta_{33}$  for the samples lie around 40pm/V. Previous work, PFM and Berlincourt, have shown that the  $d_{33}$  for the samples lies between 60 and 40pm/V, hence this result ties in very nicely.

The values of the strain induced in the sample and the calculated  $\delta_{33}$  value indicate that the sample is not being significantly clamped by the SPM cantilever. The cantilever used has a low spring constant and so is not exerting a large force on the surface of the

sample; the sample is therefore able to displace the cantilever a distance that is close to the 'open circuit' values. If the cantilever was significantly restricting the movement of the surface then the values of strain and  $\delta_{33}$  would be reduced with respect to those obtained from other techniques.

A standard hysteresis loop for a similar sample of PZT (poled positive up) is shown in Figure 6. This hysteresis loop was obtained using a Radiant Technologies P/E machine and shows all the characteristics of a standard thin film ferroelectric material. The values for piezoelectric constant (40pm/V) are very similar to those obtained using the PFM techniques. Using a similar technique employed for the 'butterfly' loops the bias in the film can be calculated due to the offset of the hysteresis loop. In this case the hysteresis loop is found to be biased towards a negative applied field by 0.94 V/ $\mu\text{m}$ . Using this figure the coercive fields for the film as analysed by the Radiant Technologies technique are -11.6 V/ $\mu\text{m}$  and 12.5 V/ $\mu\text{m}$ . The slightly higher value for the positive coercive field is expected from the arguments given earlier in this paper. The difference in the positive and negative applied fields is lower than seen for the sample probed with the SPM cantilever. There are a number of possible reasons why this might be the case, the most important one is likely to be that the sample used to generate the P/E loop had been poled. The fields used to pole the sample could be high enough to displace the charge at the interfacial region. The procedure of poling the sample may make the charge at the interface of ferroelectric material and electrode become more dispersed and therefore reside over a larger volume.

Calculation of defect concentration at back electrode-PZT interface



The offset, along the field axis, in the butterfly loops is a direct result of the imposed charge at the back electrode-PZT interface. The values of the charge density at the back electrode have been calculated for the applied biases of +/-10V. Given that;

$$E_s = \sigma / \epsilon \epsilon_0 \quad \text{Equation 1}$$

We can calculate the charge density at the interface of the PZT and electrode. By introducing the values of the known variables into Equation 1, where  $\epsilon$  is approximately 300 for PZT (30/70),  $\epsilon_0$  is  $8.85 \times 10^{-12}$  and  $\sigma$  is  $8\text{V}/\mu\text{m}$  we can determine the charge density to be  $0.025\text{Cm}^{-2}$ . This compares to a charge density of ca.  $0.3\text{Cm}^{-2}$  for the surface of poled PZT, this value is consistent with a fully charged surface. The relatively large value of the charge density at the interface compared with the surface of a fully poled and therefore charged material indicates why such large variations in the coercive field are obtained when driving the sample negatively and positively. Furthermore it is possible to determine the concentration of defects that are generating such a charge density at the electrode-PZT interface. A charge density of  $0.025\text{Cm}^{-2}$  is roughly equivalent to one unit of charge per  $6\text{nm}^2$ , or one charge for every 40 unit cells of the PZT at the interface. This assumes that the defect charge resides at or along the interface plane. As the charge concentration is likely to be associated with a defect in the crystal lattice then it is possible to assume that 2.5% of unit cells in the interfacial region are defected. The region that contains these charge defects is going to be the unit cells of PZT that are closest to the electrode-PZT interface, indeed the 2.5% of defected cells could be those that are on the interface. This large number of defects will have a very large affect on the fatigue and other fundamental properties of the sample. Other studies have shown that PZT grown in the structure examined is indeed prone to early fatigue and failure, when compared to PZT grown on electrodes that are oxygen donating. The effect of the oxygen donating electrodes is believed to reduce the number of oxygen

defects at the interface by allowing migration of oxygen during the generation of the perovskite phase.

The effect of such a large number of defected unit cells in the crystal would indicate that there is a large strain at the electrode-PZT interface. This strain will be released during cycling at fields above the coercive but the defects are unlikely to reduce in number. They are more likely to concentrate at boundaries, voids or other crystal defects where the effect will be, initially, to increase the energy required for domain reversal followed by a locking of the domains in the orientation of last the complete cycle.

## Conclusions

The paper shows that it is possible to use PFM to determine the strain behaviour of a thin film even when the surface is being displaced through only a few hundreds of pm. The sensitivity of the technique to stray fields associated with those inherent in the sample means that it is possible to make an estimate, using the displacement of the hysteresis loops, as to the number of defected unit cells that are contributing to any inherent electric bias. In this case the bias at the interface was found to be ca  $0.025\text{C/m}^2$  which relates to 2.5% of unit cells having an oxygen defect. The polarity of the bias found at the interface between the electrode and PZT was positive. This conclusion was drawn as the variation in coercive field for domain reversal shows a larger positive coercive field as compared to a negative field. The kinetics for domain reversal seem to be more dependent on the nucleation of a new reversed domain from the interface than on the absolute field applied to the film. The maximum strain that was achieved in the sample was 0.3%, with the piezoelectric constant, here quoted as,  $\delta_{33}$  is around 30-

40pm/V. Both of these values are consistent with samples that have been tested on more traditional equipment conforming to IEEE standards.

#### Acknowledgements

The author would like to thank the invaluable discussions with Dr R Dorey and J Southin (*NOTE Mike I have not added you as an Ack in case you would like to add to the paper, if not then I will, naturally, ack you*) and comments from Prof R Whatmore, Dr Q Zhang for preparing the substrate and financial support from the McKeown foundation during the research period.

#### References

1. Ramesh, R., S. Aggarwal, and O. Auciello, *Materials Science and Engineering: R: Reports*, 2001. **32**(6): p. 191-236.
2. Mikolajick, T., et al., **41**(7): p. 947-950.
3. Thiebaud, C., et al., *Annales de Chimie Science des Materiaux*, 2001. **26**(1): p. 145-149.
4. Shaw, C.P., et al., *Integrated Ferroelectrics*, 2000. **29**: p. 189-213.
5. Shaw, C.P., et al., *Integrated Ferroelectrics*, 2001. **256**: p. 159.
6. Muralt, P., et al., 1995. **29**(1-4): p. 67-70.
7. Whatmore, R.W. and R. Watton, *Ferroelectrics*, 2000. **236**(1): p. 259-279.
8. Jiang, A.Q., et al., *Journal of Applied Physics*, 2002. **92**(11): p. 6756.
9. Zhang, Q., et al., *Integrated Ferroelectrics*, 1999. **23**(1): p. 215-228.
10. Zhang, J., et al., *Solid State Communications*, 2001. **118**(5): p. 241-246.

11. Ricote, J., Q. Zhang, and R.W. Whatmore, IEEE International Symposium on Applications of Ferroelectrics, 1998: p. 483-486.
12. Luginbuhl, P., et al., Sensors and Actuators A: Physical, 1996. **54**(1-3): p. 530-535.
13. Lee, W.I. and J.K. Lee, Materials Research Bulletin, 1995. **30**(10): p. 1185-1191.
14. Zhang, Q., et al., Journal of Sol-Gel Science and Technology, 1998. **11**(2): p. 141-152.
15. Scott, J.F., Ferroelectrics, 2000. **236**(1): p. 247-258.
16. Dunn, S., A.P. De Kroon, and R.W. Whatmore, Journal of Materials Science Letters, 2001. **20**: p. 179.
17. Auciello, O., et al., MRS Bulletin, 1998. **23**(1): p. 33-42.
18. Alexe, M., et al., Applied Physics A: Materials Science and Processing, 2000. **70**(3): p. 247-251.
19. Alexe, M., et al., Applied Physics Letters, 1999. **75**(8): p. 1158.
20. Dunn, S. and R.W.W. Whatmore, Nanotechnology, 2002. **13**: p 456-459.
21. Gruverman, A., et al., Nanotechnology, 1997. **8**(3A): p. A38-A43.
22. Gruverman, A., et al., Ferroelectric Thin Films VI; Materials Research Society Symposium Proceedings, 1998. **493**: p. 53-58.
23. Huang, Z., Q. Zhang, and R.W. Whatmore, Journal of Materials Science Letters, 1998. **17**(14): p. 1157-1159.
24. Zhang, Q., R. Whatmore, and M.E. Vickers, Journal of Sol-Gel Science and Technology, 1999. **15**(1): p. 13-22.
25. Zeng, J., et al., Applied Physics A: Materials Science and Processing, 1999. **69**(1): p. 93-96.
26. Wouters, D.J. and H.E. Maes, Microelectronics and Reliability, 1996. **36**(11-12): p. 1763-1766.

27. Scott, J.F., *Ferroelectrics*, 1998. **206-207**(1-2): p. 365-379.
28. Rao, A., V, S.A. Mansour, and A.L. Bement, *Materials Letters*, 1996. **29**(December 1996): p. 4.
29. Li, A., et al., *Thin Solid Films*, 2000. **375**(1-2): p. 220-223.
30. Kim, T.S., H.-H. Park, and I.-S. Jin, *Surface and Coatings Technology*, 1998. **100-101**(1-3): p. 229-233.

## Figure Captions

Figure 1; Schematic of modifications made to a standard SPM in order to complete PFM type experiments.

Figure 2; A captured 'Scope trace' indicating the surface displacement for the sample under test at an applied sinusoidal bias of  $\pm 10\text{V}$ . The image shows the surface displacement to be ca.  $0.6\text{nm}$  and that there is very little noise introduced into the system. There is a high degree of stability in the trace which is typical of a system that has been allowed to stabilise for a period of ca. 90 cycles. The horizontal axis in the image is time or applied field to the film as the scan size was set to  $0\text{nm}$ .

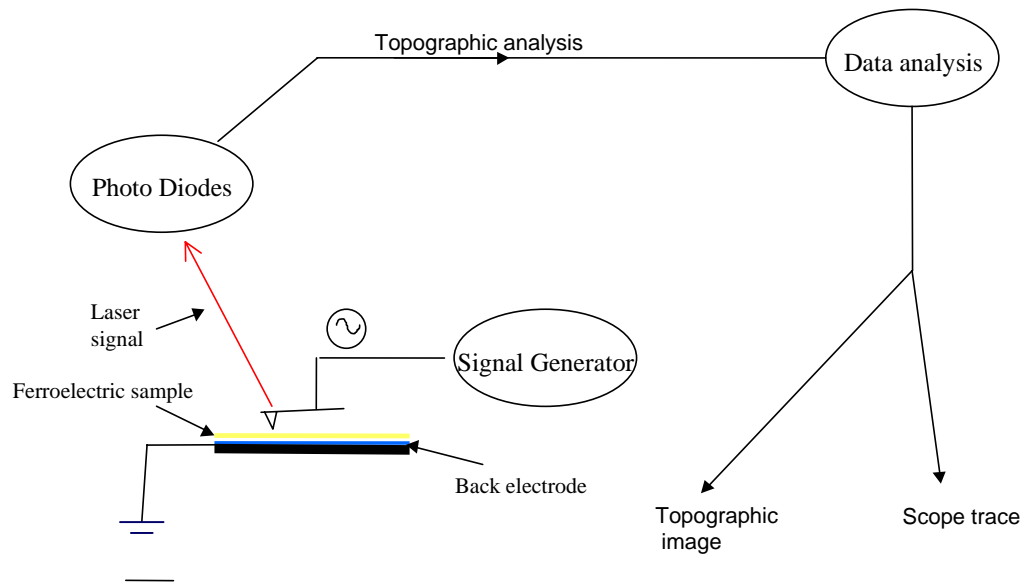
Figure 3; An SPM image of the resultant displacement of the tip for a sample showing poor tip-surface contact or poor sample grounding. The scan size is  $0\text{nm}$  and z-scale is  $25\text{nm}$ . The apparent variation in topography is a direct result of the cantilever interacting with the resultant electric field on the surface of the sample. The applied AC electric field is stepped from (at the front of the image)  $\pm 0\text{V}$  to  $\pm 10\text{V}$  (at the back of the image). Peaks in the displacement on the image coincide with peaks in the applied AC signal.

Figure 4; A captured 'Scope trace' indicating the surface displacement for the sample under test at an applied sinusoidal bias of  $\pm 7\text{V}$ . The image shows the asymmetry associated with a sample that is being driven above the coercive field in both directions of applied field. There is also more noise in the image which shows that the surface of the sample is vibrating by ca.  $300\text{pm}$ . The drift in the trace is symptomatic of a sample that has not been allowed to stabilise after adjustment of the bias. The horizontal axis in the image is time or applied field to the film as the scan size was set to  $0\text{nm}$ .

Figure 5; Strain versus field plots for PZT (30/70). The chart shows the increase in the displacement with increase in applied bias. It is possible to determine the coercive fields from this chart and at an applied bias of +10V this is shown to be +39V/ $\mu\text{m}$  and -23V/ $\mu\text{m}$  when standardised for displacement in the loops due to the internal field at the electrode-PZT interface. The absolute values of coercive field are ca 30V/ $\mu\text{m}$ . The piezoelectric constant of  $d_{33}$  can be calculated by determining the slope of the butterfly loop as it passes the zero applied field region. In this case the value is quoted  $\delta_{33}$  and lies in the region of 30-40pm/V. The maximum strain exhibited by the sample was shown to be ca. 0.3% for an applied bias of +10V.

Figure 6; A hysteresis loop obtained for thin film PZT using standard technology. Figures of 40pm/V, for  $d_{33}$ , and +/- ca.115C/cm<sup>2</sup>, for the  $C_e$ , are typical for PZT (30/70) grown in the [111] orientation on SiO<sub>2</sub>/Ti/Pt when evaluated using 'bulk' techniques.

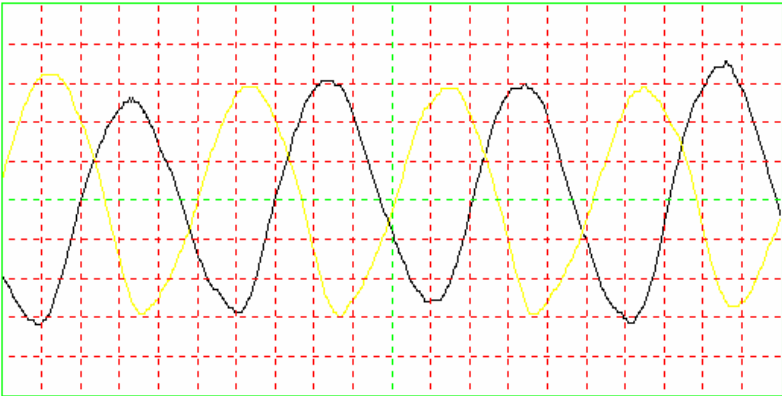
Table 1;  $d_{33}$ , coercive field values for PZT (30/70) samples measured with quasi DC PFM at various fields.

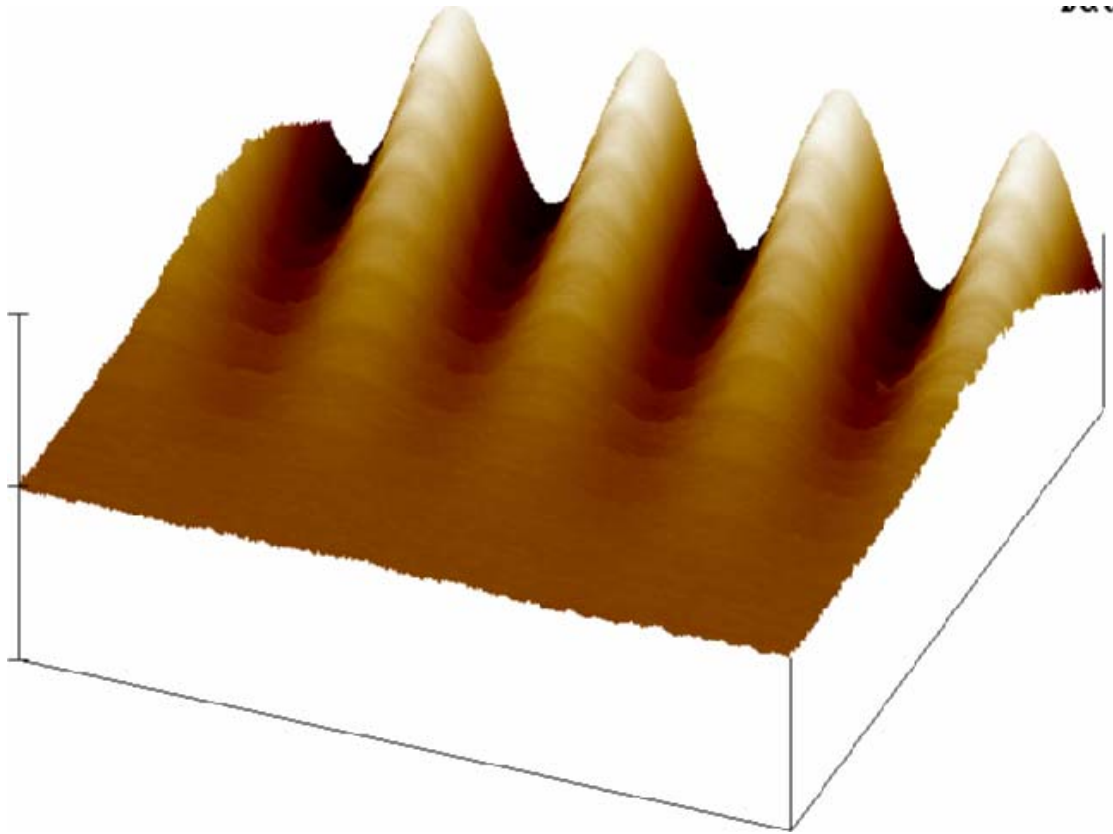




# Scope Trace

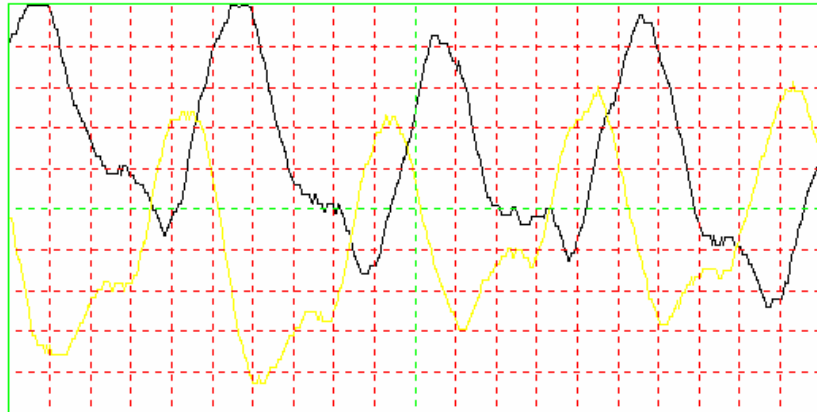
Height  
0.10 nm/div



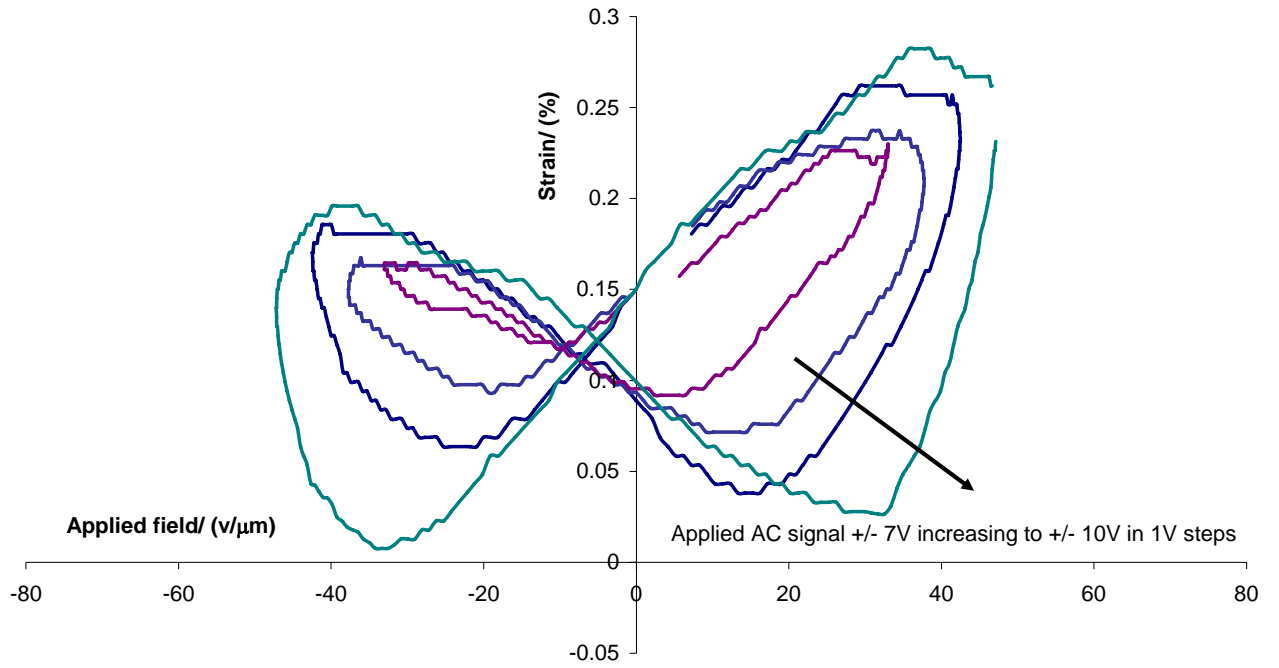


# Scope Trace

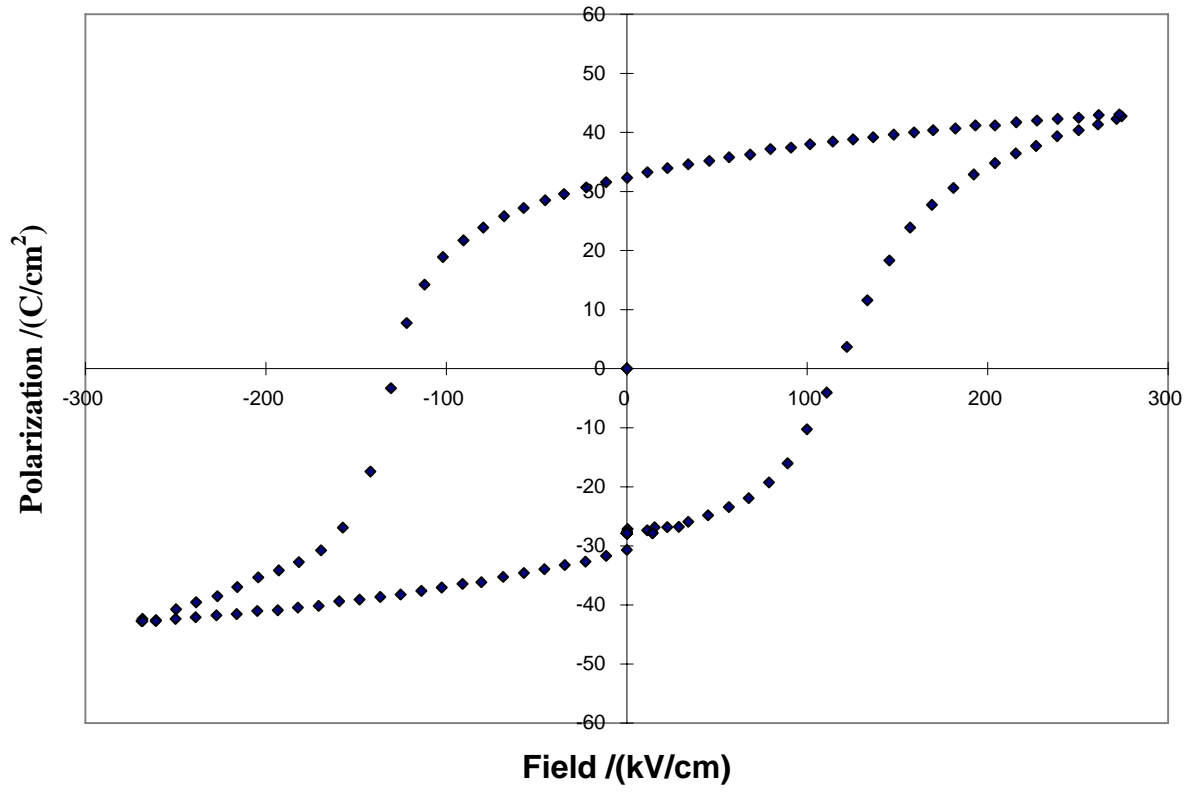
Height  
60.00  $\mu\text{m/div}$



Strain verses applied field for PZT (30/70)



### PZT (30/70)



Applied voltage	$\delta_{33}$ /(pm/V)	+ coercive field/ (v/ $\mu\text{m}$ )	- coercive field/ (v/ $\mu\text{m}$ )
7	30	8	n/a
8	28	16	18
9	36	16	24
10	41	32	30